International Journal of Environmental Sciences
ISSN: 2229-7359
Vol. 11 No. 23s, 2025
https://theaspd.com/index.php

Heat Transfer Enhancement of Two-Phase Flow with Turbulent Promoters

Shoaib Abdul Samad Dhansay[1], Dr. M.D. Hambarde[2], Dr. Chidanand[3] D. Koshti[4]
[1]M. Tech Student, Thermal Engineering, Department of Mechanical Engineering, Dr Vishwanath Karad MIT World Peace University, Pune, Maharashtra
[2]Assistant Professor, Department of Mechanical Engineering, Dr. Vishwanath Karad MIT World Peace University, Pune, Maharashtra
[3]Assistant Professor, Department of Mechanical Engineering, Dr Vishwanath Karad MIT World Peace University, Pune, Maharashtra

Abstract
This study investigates the enhancement of two-phase heat transfer in refrigeration system using turbulent promoters, specifically twisted tape and perforated twisted tapes. The heat transfer enhancement with respect to vapor quality during the flow boiling of R-407C is investigated using twisted tape inserts in a horizontal tubular evaporator with an inner diameter of 13.40 mm and a length of 2 meters. This study looks at how things work when the heat flux is between 3 and 9 kW/m², the mass flux is between 120 and 280 kg/m²·s, and the working pressures are 3, 5, and 7 bar. The void fraction of the air ranges from 0.05 to 0.95. The data show that as the quality of the gas improves, the heat transfer coefficient also improves, especially at higher pressures. The performance of heat transfer is greatly improved when twisted tape pieces are used, especially in areas with lower air quality. The average improvement in heat transfer seen with twisted tapes was between 35% and 60%. At 7 bar pressure, the best performance was seen. When you compare twisted tape to perforated twisted tape, you can see that twisted tape inserts improve heat transfer the most, which makes them perfect for evaporative cooling uses. The study comes to the conclusion that twisted tape pieces are especially helpful for improving heat transfer when the air quality and pressure are higher.
Keywords: *Heat Transfer Enhancement, Two-Phase Flow, Turbulent Promoters, Perforated Twisted Tapes, Refrigerants, R407C*

I. INTRODUCTION

Heat transfer enhancement in two-phase flow systems is a critical area of research in the fields of refrigeration, air-conditioning, and power generation[1]. When used for heat exchange, "heat exchangers" mean that the efficiency of the heat exchangers, drums, and condensers is what makes the system work well as a whole. Heat exchanges make it easier to move heat from one flow of liquids to another. Improving the efficiency of thermal systems continues to be a high priority, since this allows for decreased energy consumption and improved thermal control, and ultimately decrease environmental impact, as the world continues to expand its energy consumption. Two-phase - a flow regime with both liquid and vapor phases is a traditional flow regime part of refrigeration cycles as the phase change processes are very important in heat exchange [2].

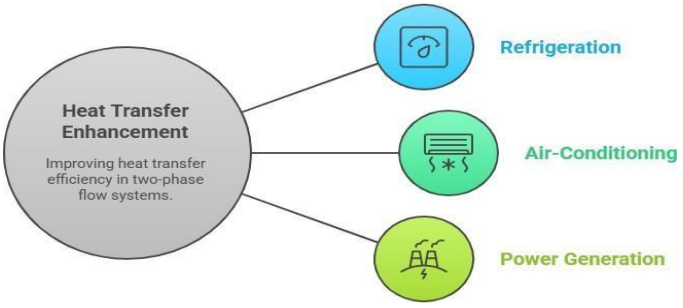

Figure 1: Enhancing Heat Transfer in Two-Phase Flow Systems

Disruptive promoters, such as twisted tape and long length perforated twisted tapes, are often used to increase heat transfer in a flow through the turbulence they induce in the flow. Disruptive promoters alter the thermal boundary layer, increase fluid mixing and the convection heat transfer, resulting in a

large gain of performance [3]. Out of all of these tools, open twisted tapes have gotten the most attention because they can improve mixing and lower flow resistance. Also, when used in a two-phase system, these devices provide better heat transfer by altering the flow characteristics, while not creating large pressure losses, leading to opportunities for applications that require high heat transfer with low energy costs [4].

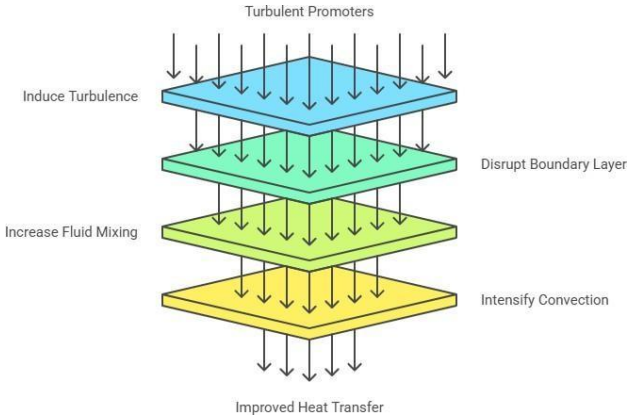

Figure 2: Enhancing Heat Transfer Efficiency

As seen in Figure 2, turbulent promoters enhance heat transfer efficiency by introducing turbulence, penetrating the thermal boundary layer, increasing fluid mixing and convection, all enhancing heat transfer [5]. Air cooling systems use coolants like R407C to keep things cool. This can be both a problem and an opportunity when it comes to heat transfer efficiency. R407C represents excellent thermal performance in combination with low Global Warming Potential (GWP) and positive environmental outcomes. The research within scrutinizes thermal performance of these refrigerants investigated with the turbulent promoters to review to impact heat-transfer mechanisms, refrigerant properties and enhancement device designs [6]. The goal is to optimize heat transfer performance while maintaining system efficiency and sustainability, paving the way for next-generation refrigeration technologies[7].

II LITERATURE REVIEW

Using less energy and having less of an effect on the world are both good goals, but the best way to reach these goals is to make heat flow better in cooling systems. Nano-refrigerants and improved models are two new ideas that have been written about as ways to improve heat movement in refrigeration systems.

Hambarde et al. (2017) an experiment that looks at how R407C evaporates in a single straight horizontal tube. This research extensively examined the movement of heat through R407C while varying the temperature slide, vapor quality, mass flow, and heat flow. The study was undertaken in variable operating conditions to provide additional understanding of the heat transfer coefficient during flow boiling which presents useful data to encourage the application of R407C as a suitable alternative to R22 in domestic refrigeration applications [8]**. Hambarde et al. (2019),** investigates how heat transport might be aided by twisted tapes in a tube evaporator during the flow boiling of R407C. This study investigates the impact of altering the operating parameters of heat flux, void fraction (vapor quality), evaporation temperature, and mass flow. The results showed that a void percentage between 10% and 40% significantly improved heat transmission. The optimum heat transfer improvement was from twist ratios of 12, 10 and 8 with all improvements corresponding to a twist ratio of 12. This work provides a better understanding of the effects of turbulent promoters on the heat transfer performance of refrigerant applications [9]. **Hambarde et al. (2018),** examines the heat transfer behavior of twisted tape inserts during the evaporation of R407C in a plain horizontal copper tube. Different levels of mass flow, evaporation pressure, heat flux, and vapor quality were used in the tests. In the 10% to 50% vapor quality range, twisted tape plugs improved heat transfer.

This was tested for three different twist ratios (y = 8, 10, and 12). y=12 improved heat transfer the most, followed by y=10. The study also looks at how shape and working factors affect how well twisted tapes move heat [10]. **Bilen et al. (2024)** conducted an experiment in the lab comparing the impact of R134a and R1234yf, two nano-refrigerants, on vapor-compression refrigeration systems. Graphene, CNT, and AlO_0 nanoparticles were added and combined in R1234yf to greatly enhance the vapor-compression refrigeration system's (VCRS) performance. When graphene nanoparticles were added to pure refrigerant

R1234yf, their cooling capacity increased by 24% on average, and their Energy Efficiency Ratio (EER) increased by 32% [11].

Deb et al. (2023) examined the R407C refrigerant's boiling and flow in horizontal, smooth micro-fin tubes. Micro-fin tubes performed better than smooth tubes in terms of heat transfer rate, as shown by the author's experiment. This illustrates the importance of surface modification in heat exchangers [12]. **Kim (2020)** Convective boiling of R-410A in micro-fin tubes with 5.0 mm and 7.0 mm outer diameters was investigated. The research found that a smaller tube had a higher enhancement factor. For example, the 5.0 mm tube showed an enhancement factor between 1.63 to 3.26. Because of this, the tube's heating capacity is greatly increased by decreasing its diameter. **Diani et al. (2021)** R1234ze (E)'s boiling performance was assessed using two distinct tube types: a micro-fin tube of the same size and a smooth tube with a 2.5 mm ID. In every situation, but particularly when the steam quality was higher, the micro-fin tubes performed better than the smooth ones. This happened as a result of better convective boiling caused by the design of the micro-fin tubes [13]. **Mancin et al. (2022)** Using a micro-fin tube with an outside diameter of 7.0 mm, researchers studied the boiling and flow characteristics of R450A, R515B, and R1234ze (E) refrigerants. The study expanded our understanding of low-GWP refrigerants by showcasing their potential as environmentally beneficial alternatives to traditional refrigerants [14]. **Nalbandian et al. (2022),** In a microchannel-rich extruded aluminum tube, flow boiling heat transfer tests were performed on the HFO-1234yf and HFC-134a refrigerants. The authors used experimental data to show how changes in mass velocities and vapor characteristics affected the two refrigerants' heat transfer coefficients. The scientists found that when employed as a coolant, HFC-134a consistently performed up to 22% better than HFO-1234yf. It was also shown that heat transfer was very mode-dependent. The authors successfully compared low-GWP alternatives to traditional refrigerants in microchannel heat exchangers. Environmentally friendly car air conditioners may benefit from utilizing low-GWP refrigerants, as shown here [15].

Vidhyarthi et al. (2024), investigates the flow boiling and heat transfer of R134a refrigerant via micro-fin tubes. Test results have been compared between straight tubes and micro-fin tubes. According to the findings of many studies, micro-fin tubes performed up to 270% better in heat transmission than smooth tubes. According to the trials' findings, micro-fin tubes have a promising future in the HVAC industry and may enhance performance by lowering lubricating nucleate boiling and dry-out. By contrasting experimental results with pre-existing models, it is verified. The authors demonstrate that the micro-fin shape enhances heat exchanger performance and that there is sufficient agreement and correlation with the models [16]. **Hamid et al. (2022),** looks at how HFO-1234yf and HFC-134a perform in rectangular channel microchannel heat exchangers with regard to pressure drop performance or flow boiling heat transfer properties. Depending on the mass in motion and the quality of the gas, the findings reveal that HFC-134a outperforms HFO-1234yf by a heat transfer coefficient ranging from 0.2 to 22%. This work elucidates the parameters affecting the efficiency of HFO-1234yf refrigerants in microchannels of tiny diameters, used in automotive air conditioning systems, by demonstrating that the heat transfer characteristics of these refrigerants are significantly influenced by the flow pattern and vapor quality [17]. **Dang et al. (2011),** contrasts the efficacy of HFO-1234yf and HFC-134a in transferring heat when boiling in horizontal tubes. The results indicate that HFO-1234yf and HFC-134a had comparable heat transfer coefficients. In other flow tests, nevertheless, HFC-134a did better than HFO-1234yf. The findings indicate a promising potential for HFO-1234yf as a low-GWP substitute for HFC-134a in refrigeration systems; however, further investigation is required to thoroughly understand its thermophysical properties, its behavior in microchannels for heat transfer, and its efficacy across diverse HVAC applications [18].

Saito et al. (2011), while boiling in tiny tubes, scientists studied the heat transfer properties of HFO-1234yf and HFC-134a. Depending on the heat transfer scenario, the findings demonstrated that both refrigerants perform similarly in terms of heat transmission. Both refrigerants have their heat transfer mechanisms discussed in relation to gas quality and mass flow. Though this study suggests that HFO-1234yf might be a good alternative refrigerant, there is a lack of data that would allow for its full use in commercial HVAC systems. Note that the shift in the testing environment is another possible source of discrepancy in the findings [19]. **Longo et al. (2019),** provides experimental measurements of flow boiling heat transfer for refrigerants HFO-1234yf and HFC-134a in a smooth copper tube with a diameter of 4.0 mm[20]. When vapor quality is poor, the heat transfer coefficients of the refrigerants are almost identical, according to the research. On the other hand, HFC-134a has superior heat transfer capabilities in

situations when the vapor quality is elevated. According to the authors, more research is required to fully understand the characteristics of HFO-1234yf, particularly at high heat fluxes, and to find ways to make this refrigerant more eco-friendly for future cooling applications. **Sempértegui-Tapia and Ribatski (2017),** The results showed that HFO-1234yf has higher heat transfer coefficients at lower heat fluxes, while HFC-134a has higher heat transfer coefficients at higher heat fluxes, thus showing a favorable result for HFC-134 [21]. Further testing in a larger tube is necessary to quantify the performance differences between the two refrigerants in various cooling applications, but the study did find that HFO-1234yf is a reasonable replacement for HFC-134a, especially in low-GWP refrigerant applications. **Yang et al. (2018),** examines the transfer of heat from boiling HFO-1234yf and HFC-134a via a 4-millimeter-wide cylindrical tube. According to the results, HFO-1234yf is not as effective at transferring heat as HFC-134a, on average. The discrepancy is meaningless in terms of flow conditions [22]. When heated to boiling, the efficiency with which these two refrigerants transported heat varied greatly.

Li et al. (2021) investigates how heat is transferred from boiling HFO-1234yf down a horizontal tube that is 2.0 mm wide, modifying the mass velocities and heat fluxes as necessary. The heat transfer coefficients of HFO-1234yf rose dramatically as the mass velocities and vapor quality improved. The research determined that heat transfer rates were optimal when the flow was moving uphill, after examining the effect of slope angle. In sum, the research clarifies HFO-1234yf's flow boiling performance to a high degree, which is an important step in realizing the refrigerant's promise as a greener option for next-gen cooling systems [23]. **Zhang et al. (2022)** The flow boiling heat transfer capacities of R410A have been studied in horizontal circular channels with improved microporous, ring-shaped finned, and small bossed tubes. The microporous tube was clearly superior to the smooth tube, with heat transfer rates up to 2.64 times greater. The upgraded tubes' enhanced heat transmission was a result of the altered bubble form brought about by the curvier streamline, as opposed to the smooth tube's equivalent. Consequently, the enhanced tubes allowed the bubble to move heat more rapidly and with less resistance during flow boiling. It was simpler to foretell the trials' outcomes thanks to the new connections presented in the article. With better tubes, these estimations were within ±2% and smooth tubes, within ±10%, indicating a higher level of accuracy [24]. **Zhang et al. (2025)** Experimental flow boiling heat transfer was examined for smooth tubes with varying tube slope angles ranging from 0° to 90° in a comparative study. In particular at lower vapor quality regimes, this study found that the distribution of the vapor-liquid phases was not uniform. It also discovered that dry-out behavior and Departure from Nucleate Boiling (DNB) were two kinds of boiling crises that occurred. The coefficients of heat transmission and frictional pressure drop were significantly impacted by the thrust angle [25].

Li et al. (2024) In a micro-fin tube, we observed the stacking and boiling behavior of R32 with somewhat miscible POE oil. They discovered that layering the mixture improved heat transmission compared to entirely mixing the oil. Because the micro-fin tube displayed layers of oil-rich and oil-poor components during the stratification flow, heat transmission was improved. An overall improvement in energy efficiency and a new heat transfer equation that predicted 91% of the outcomes were the end outcomes [26]. **Jadhav et al. (2021**) examined the quantity of pressure loss that transpired when R-407C was boiled in a horizontal tube with a bent tape insert. The two studies showed that pressure drop reduces with increasing tube tilt and rises with increased gas quality. They discovered that using twisted tape plugs improved the efficiency of flow boiling in a horizontal tube. They created models to predict pressure drops as an extra service, which designers might use to build cooling systems that work better [27]. **Tarabkhah et al. (2023),** Using machine learning algorithms (ANN, SVR, KNN, and XGBoost), they calculated the frictional pressure drops (FPDs) and heat transfer coefficients (HTCs) for R1234yf and R134a in both horizontal and vertical tubes under condensing circumstances. With a MAPE of 7.01%, the ANNMLP prognosis was the best for HTC, while XGboost's forecast was the best for FPD, with a MAPE of 10.87%. The findings demonstrated that the mass motion and slope angle had a substantial impact on the FPD and HTC [28]. **Li et al. (2020)** evaluated the ability of three distinct improved tubes—tiny bosses, integral-fin, and micro-porous—to transmit heat when R410A was boiling. With a coefficient that was 2.5–2.6 times greater than the smooth tube's, the microporous tube performed better in terms of heat transfer. As expected, it was shown that modified tubes improve heat transfer efficiency and provide new correlations that allow for precise heat transfer coefficient prediction in a variety of flow conditions [29].

Table 1: Literature survey

Authors	Refrigerant(s)	Enhancement Technique	Parameters Tested	Key Findings
Bilen et al. (2024)	R1234yf with nanoparticles	Nano-refrigerants	Cooling capacity, EER, compressor power input	0.25% graphene addition improved EER by 32% over pure R1234yf.
Deb et al. (2023)	R407C	Micro-fin tubes	Heat transfer coefficient, pressure drop	Micro-fin tubes enhanced heat transfer compared to smooth tubes.
Kim (2020)	R-410A	Micro-fin tubes (5.0 mm & 7.0 mm OD)	Enhancement and penalty factors, mass flux	Smaller diameter tubes showed higher enhancement factors in convective boiling.
Diani et al. (2021)	R1234ze(E)	Smooth vs. micro-fin tubes	Heat transfer coefficient, vapor quality	Micro-fin tubes outperformed smooth tubes, especially at higher vapor qualities.
Mancin et al. (2022)	R450A, R515B, R1234ze(E)	Micro-fin tubes	Boiling mechanisms, heat transfer characteristics	Alternative refrigerants demonstrated effective boiling performance in micro-fin tubes.

III. EXPERIMENTAL SETUP

3.1 : Experimental setup layout

As per the objective of the research, for experimental investigation, a schematic layout of the refrigeration vapor compression system setup is shown in the figure below:

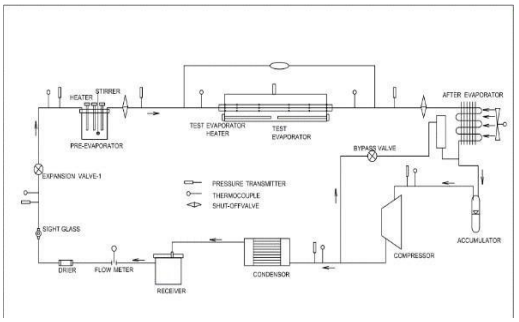

Figure 3: Experimental Setup

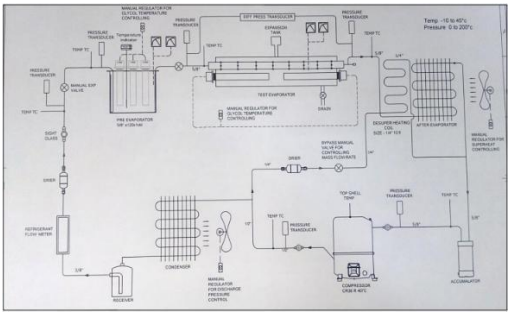

Figure 4: Experimental Setup for fabrication

3.2 : Fabrication of Experimental Setup Component

3.2.1 Pre-Evaporator

As shown in Figure, the pre-evaporator consists of a copper tube coiled around a stainless steel drum. This soft copper tube is shaped into a coil with an outer diameter slightly (2 mm) smaller than the drum's inner diameter. It enters the drum at the top, coils downwards to the bottom, and then returns upward in the same coiled fashion. Both ends of the coil are connected to 19.05 mm (3/4" diameter), 0.5 mm thick headers. The real-life picture of the pre-evaporator is shown in Figure 3.3(b). It has a drum that is 500 mm in diameter and 700 mm tall. There is a mix of 30% ethylene glycol or 70% water in the drum. Three electric rod heaters, each with 3 kW of power, are submerged in this fluid to heat the copper coil that holds the refrigerant. An electric mixer in the middle of the drum makes sure that the heat is spread evenly across the coil surface by moving the fluid mixture around. Figure 3.3(d) shows how the copper coil is made inside the drum, while Figure 3.3(a) shows the heaters and stirrer in their places from above. The drum is wrapped in rubberized nitrile foam rubber padding to keep heat from escaping after the stirring, motor, and heated elements are put in place. A solid-state switch and a PID processor work together to precisely control how much heat goes into the pre-evaporator.

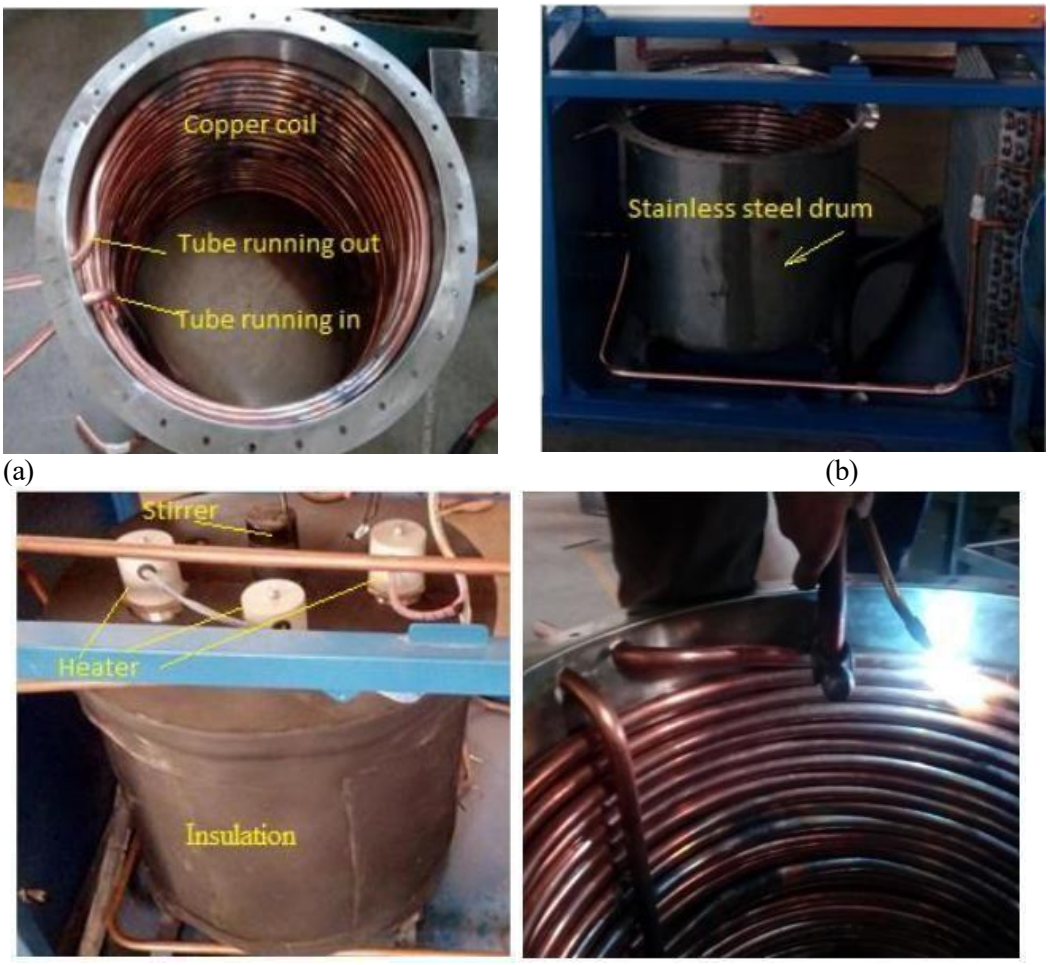

(a) (b)

(c) (d)

Figure 5: Pre-Evaporator

Table 2: Technical specifications of Pre-Evaporator

Material of tube	**Copper**
Length of coil	6 meters
Surface area of coil through which fluid flows	0.2523 sq. m
Inner Dia of coil	13.386 mm
Outer Dia. Of coil	15.875 mm

3.2.2 : Test-Evaporator

As shown in Figure 3.4, the test evaporator is constructed as a tube-in-pipe system. In this setup, a copper test tube is inserted inside a horizontal stainless-steel pipe that measures 100 mm in internal diameter, 103 mm externally, and spans 2 meters in length. At the centre of this horizontal pipe, a 200 mm long vertical pipe having the same diameter as the main pipe is welded. This vertical section functions as a filling header for the water-glycol mixture and is sealed at the top with a stainless-steel cap. Both ends of the horizontal pipe are closed using flanges that are custom-built to allow the insertion of the copper test tube and heating rods. Figure 3.4 illustrates the layout of the test evaporator, highlighting components like the horizontal and vertical pipes, flanges, test tube, heating rods, and provisions for inserting turbulent promoters. Two electrical heating rods each 0.9 meters long and rated at 1 KW are installed from both ends of the horizontal pipe using the flange mounts, as shown in Figure 3.4(a). These heaters ensure that heat is applied uniformly across the length of the copper tube, enabling consistent thermal conditions. The heat input is precisely managed using a solid-state relay controller.

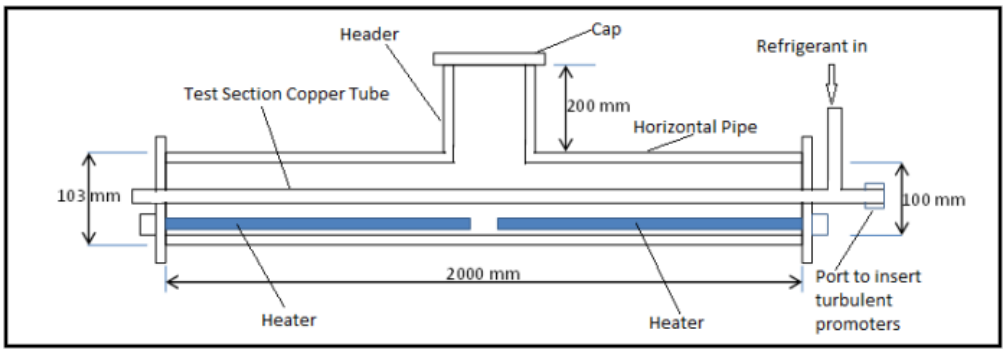

Figure 6: Schematic of Test-Evaporator

Table 3: Technical specifications of Test-Evaporator

Material of tube	**Copper**
Length of test section	2 meters
Mass flux (Kg/m^2 s)	100 to 350
Heat Flux (KW/m^2)	2 to 10
Evaporator Pressure	3 to 8 bar
Evaporative Temp.	-15 °C to 15° C
Area Of tube	0.00014082 m^2
Inner Surface Area	0.084 m^2
Outer Surface Area	0.0997 m^2

3.2.3 : Test-section copper tube

The basic layout of the copper tube test section is shown in the figure. A copper tube that is two meters long and has an exterior width of 15.88 mm and an interior diameter of 13.39 mm is the test item. To measure the average outer surface temperature of this tube, a total of 16 thermocouples are affixed by brazing onto its outer surface. These thermocouples are distributed across six equally spaced positions along the length of the tube. At each of these positions, four thermocouples are mounted, spaced 90 degrees apart around the tube's circumference.

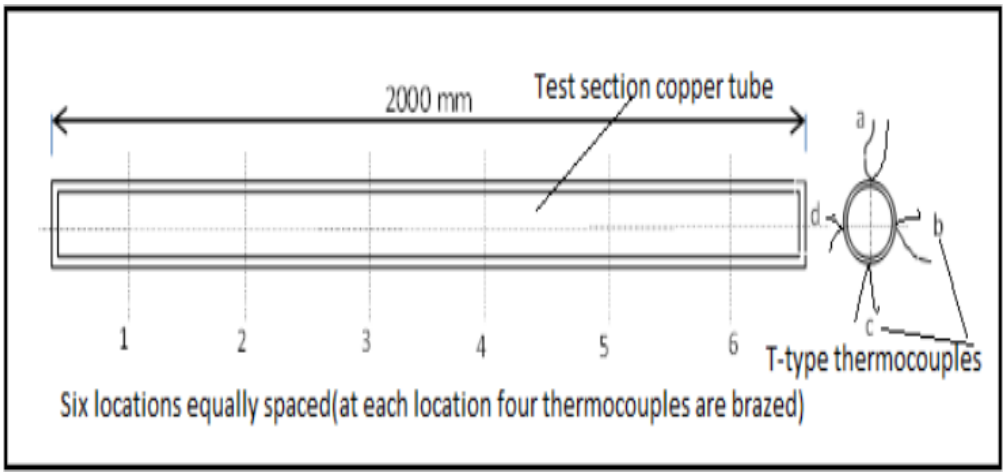

Figure 7: Schematic of Test-Section Copper Tube

3.2.4 After-Evaporator

For a refrigeration system that uses vapor compression, an experimental setup was created. The system uses a manual expansion valve in conjunction with a bypass valve to accommodate changes in mass flow and pressure, rather than a thermostatic expansion valve. The working conditions in the test section change all the time, especially the mass flux and heat flux. This means that the refrigerant might stay wet at the test evaporator's exit or the compressor's intake. This can lead to wet compression, which hurts the performance of the compressor and could even cause it to break down. It is very important to make sure that the refrigerant going into the compressor is almost completely dry and soaked as a mist. This is checked with the compressor superheat, which is the difference in temperature between the refrigerant's

real temperature at the compressor inlet and its saturated temperature at the intake pressure. Standard practice in cooling says that this superheat shouldn't be higher than 7 K. To achieve this, an after-evaporator is installed between the test evaporator and the compressor. This component helps maintain the necessary superheat level before the refrigerant enters the compressor. For the 2.5 TR experimental system, an after-evaporator is fabricated with suitable specifications.

Figure 8: After-Evaporator

3.2.5 Compressor

The Compressor is selected as per the following Specifications:

Table 4: Technical specifications of Compressor

Manufacturer	Emerson Climate Technologies (India) Private Limited
Model	CR35K6ME-TFM-121DM
Compressor type	Hermetically sealed, Reciprocating, Connecting Rod type
Refrigerant	R407C
Application Group	High Temperature
Evaporating Temp. Range	-23 C to 12.8 C
Cooling Capacity	Nominal HP-2.35
Rated Voltage	380 - 420V, 50Hz, 3 Phase

Figure 9: Compressor

Figure 10: Complete Setup

3.2.6 Perforated twisted tapes

Heat exchangers, which are usually made of copper because it conducts heat well, use perforated twisted tapes to help the heat move through them. These tapes are made of metal strips twisted along their length with holes at equal intervals. Twisting the metal creates a helical fluid flow, which introduces turbulence that enhances mixing and disrupts a \A-bndry layer close to the tube surface, thereby increasing heat transfer. The holes in the tape also increased mix of flow and created local vortexes that provided added stimulation for heat exchange, as well as preventing stagnant zones which lower performance. The copper in the doughnut heaters is treated to withstand corrosion and has excellent thermal properties enabling these fins to be used in refrigeration and heat exchanger systems. The twist and perforation allow for favourable lower energy consumption outcomes, as well as improved heat transfer, stable operational qualities at high flows making them a viable solution in high temperature applications.

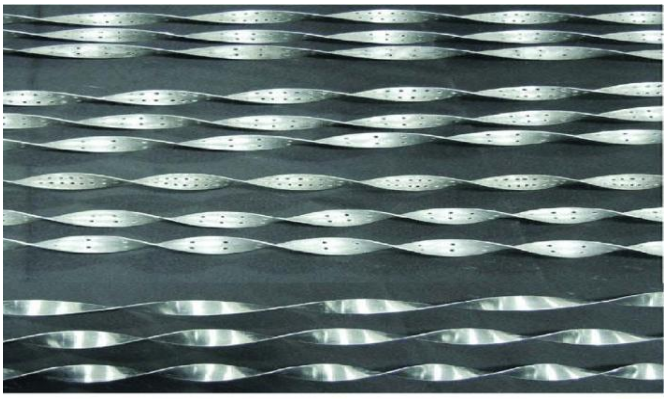

Figure 11: Perforated twisted tape (copper)

IV. METHODOLOGY & TESTING PARAMETER

The first step was to carry out the system leak test by introducing nitrogen gas into the system and holding it at 280 PSI for 48 hours. During the test process, only a minimal amount of pressure did drop evidencing that no substantial leaks were present. A vacuum test was also undertaken and confirmed that no leaks existed. Once this step was completed the liquid line isolation valve (upstream of the evaporator) was opened and the vapor compression system was operational. First of all, when the system was powered on a check for operational status, including the compressor, condenser fan and after-evaporator fan were initiated. Once the system reached stable operation, the manual expansion valve was adjusted to obtain the target operating evaporative pressure and evaporative temperature. The pre-evaporator and test-evaporator heaters were turned on after, while ensuring that the fan speed was kept at reasonable levels regarding the required superheat levels, between 50°C and 100°C are most beneficial for protecting compressor operation; that is, referring back to cautioning against compressor re-flux. These actions were undertaken to ensure there was an operationally reliable experimental set up, to complete the testing and data collection as planned.

4.1 Validation of Experimental Setup:

The researchers used the refrigerant R407C in a single-phase trial to make sure that the equipment they were using was accurate and could be used again and again. The single-phase heat transfer coefficients that were measured in the lab were then compared to the numbers that the Dittus-Boelter correlation said they should be. This widely accepted empirical association was one of the first models made for how

heat moves through turbulent flow in smooth tubes.

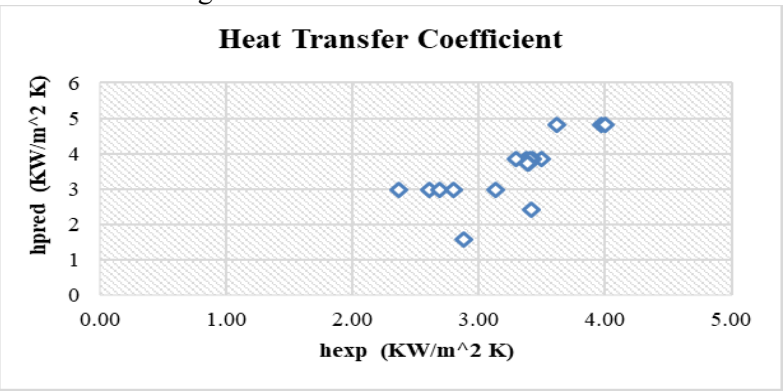

Figure 12: Validation of system

4.2 Design of Turbulent Promoters

Twisted and perforated twisted tapes are examples of enhancement devices. The holes on the tapes are particularly designed to lower flow resistance and encourage mixing. Using a hybrid technique, this study assesses the heat transfer performance of R407C with turbulence promoters by integrating experimental analysis. To encourage turbulence and phase interaction, twisted tapes (including perforated twisted tapes) were used as enhancement devices. The test rig consists of a heated horizontal test tube with instrumentation for measuring thermal performance.

Material	**Copper**
Length	2000 mm
Twists	16,18,20
Twist Ratio's	7,8,9

Table 5: Technical specifications Turbulent Promoters

Avg. mass density (ρ)	1230 kg/m^3
Thermal conductivity of the fluid (K)	0.084
dynamic viscosity of fluid (μ)	0.0002097
specific heat of the fluid at constant pressure (Cp)	1409

V. RESULTS & DISCUSSION

Experimentation was conducted in two parts:

- Part A looks into how heat moves, the pressure drops, and the temperature changes as R407C evaporates in a flat, horizontal tube.
- Part B looks into how to improve heat transfer overall while R407C evaporates in a flat, horizontal tube using turbulent promoters.

5.1 Heat Transfer Coefficients at Different Operating Conditions

Table 6 displays the investigations on R407C flow boiling in a horizontal tube. It contains information on various workplaces. The following are some of the numbers that were tallied: It shows the heat flow (q), the average pressure (Pavg), the wall temperature (Tw), the pressure going in (P1), the pressure going out (P2), the temperature going in (T1), the temperature going out (T2), and the total heat transfer rate (Q). For each case, the table also shows the expected (hpred) and observed (hexp) heat transfer factors.

Table 6: Operating Parameters with Range for Experimentation

Parameters	Range
Refrigerant mass flux, **G** (Kg $m^{-2} \cdot s^{-1}$)	120 – 280
Heat Flux, **q** (kW m^{-2})	3 – 7
Temperature range at inlet to evaporator test section (°C)	17.1 – 24.4
Pressure range (absolute) at inlet to evaporator test section (bar)	3 - 8
Vapor quality, **x**	0.1 – 0.95

The initial section investigates the evaporation of R407C in a horizontal tube. It includes the heat transfer coefficient for flow boiling, pressure decline, and temperature gliding. The evaporation of R407C in a straight horizontal conduit with varying mass and heat flux levels has been the subject of a variety of investigations. The following are the results. The evaluations encompassed the boiling heat transfer coefficient, vapor quality, pressure decline, and temperature glide. The data is presented in the following manner:

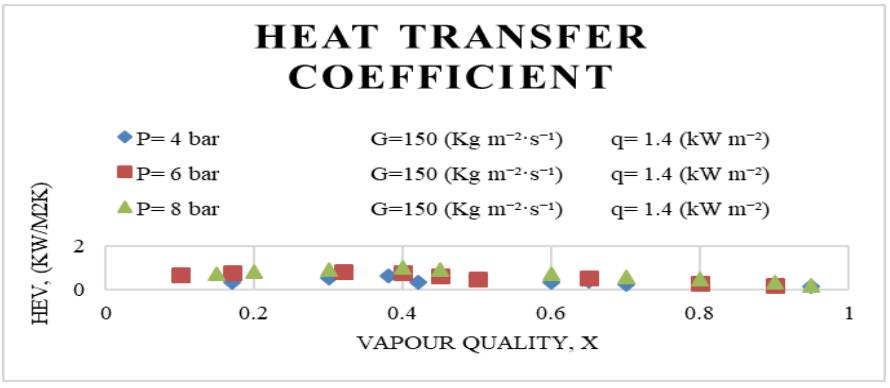

Figure 13: Heat Transfer Coefficient vs. Vapour Quality at Different Bar Pressures

The vapor quality (x) and heat transfer coefficient (hev) at 4, 6, and 8 bar pressures are shown in these graphs. maintaining a constant 1.4 kW m⁻2 heat input and a 150 kg m⁻2·s⁻* mass input. As anticipated, poor air quality (x < 0.4) resulted in relatively low heat transfer coefficients. Additionally, the results showed that at 4 and 6 bars, the heat transmission coefficients differed. As air quality improved, the heat transfer coefficient increased significantly. Four and six bar increases were larger than eight bar increases. At 6 bar and 8 bar, an exponential form that seems to be beneficial suggests that heat transfer performance may be improved with increased pressure, and that it is also positively affected by better liquid quality. It seems that the heat transfer coefficient performs better at greater pressures, making it more suitable for uses requiring a higher quality of vapor. On the other hand, it's not ideal for uses where the heat transmission efficiency varies over stages of operation.

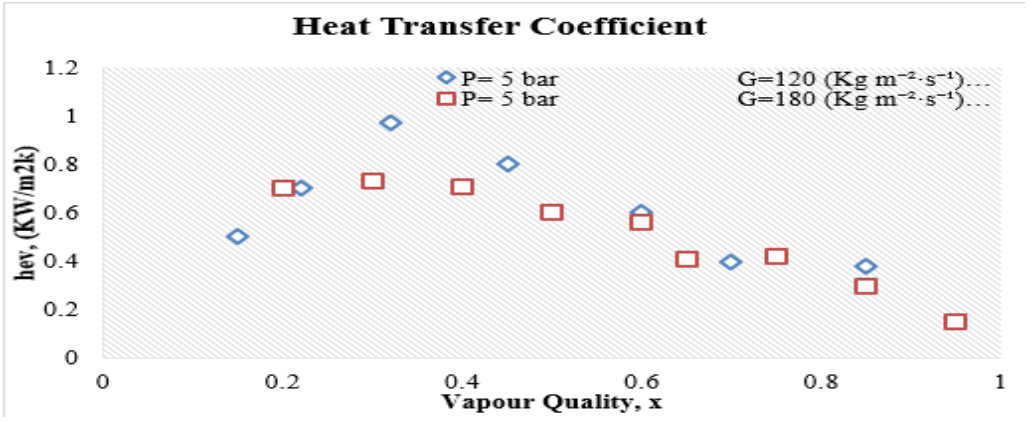

Figure 14: Heat Transfer Coefficient vs Vapour Quality

The graph shows the relationship between heat transfer coefficient (hev) and vapor quality (x) at 5 bar pressure and 2.1 kW m⁻2 heat flux. Mass flow rates per second may be 120-180 kg/m*. After rising with vapor quality, the heat transfer coefficient now rises at intermediate vapor quality. That is more evidence that heat transmission is more effective when a substance changes from a liquid to a gas. However, after a while, the heat transfer index begins to decline, indicating that as air quality improves, the rate of heat transmission slows down. Although the basic trajectory is consistent, the heat transfer coefficient shows

small differences throughout pressures. Data for varied pressures are represented by the several indicators.

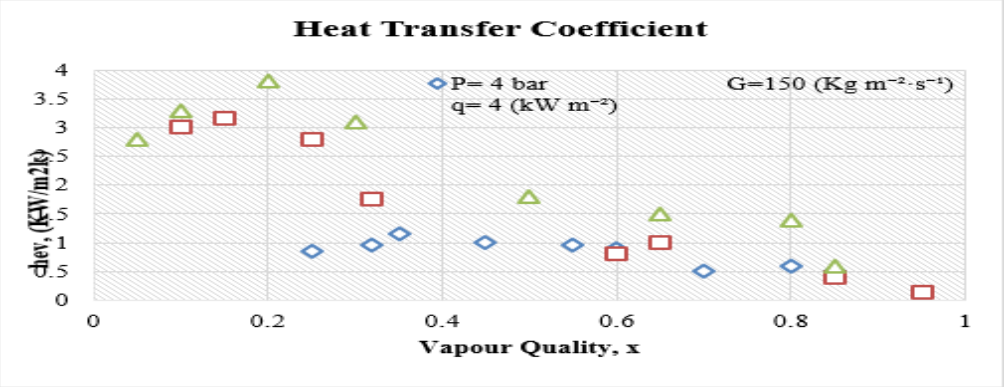

Figure 15: Heat Transfer Coefficient vs. Vapour Quality

As the pressure goes from 4 to 8 bar, the mass flow goes from 150 kg m⁻2·s⁻2 to 250 kg m⁻2·s⁻2, and the heat flux goes from 4 kW m⁻2, the changes in the gas quality and heat transfer coefficient (hev) become apparent. When the gas quality is between 0.05 and 0.2, the heat transfer rate goes up by a huge amount. At a gas quality of 0.2, it has a value of 3.8. This first rise shows that lower-quality air makes it easier for more heat to move. When the air quality is between 0.2 and 0.3, the heat transfer index goes up a little but stays around 3.1. The heat transfer rate, on the other hand, starts to go down when the liquid quality hits 0.3. In the area with better vapor quality, from 0.6 to 0.95, there is a change from 0.5 to 1.8. Most likely, these changes are caused by the move from nucleate boiling to less efficient types of boiling.

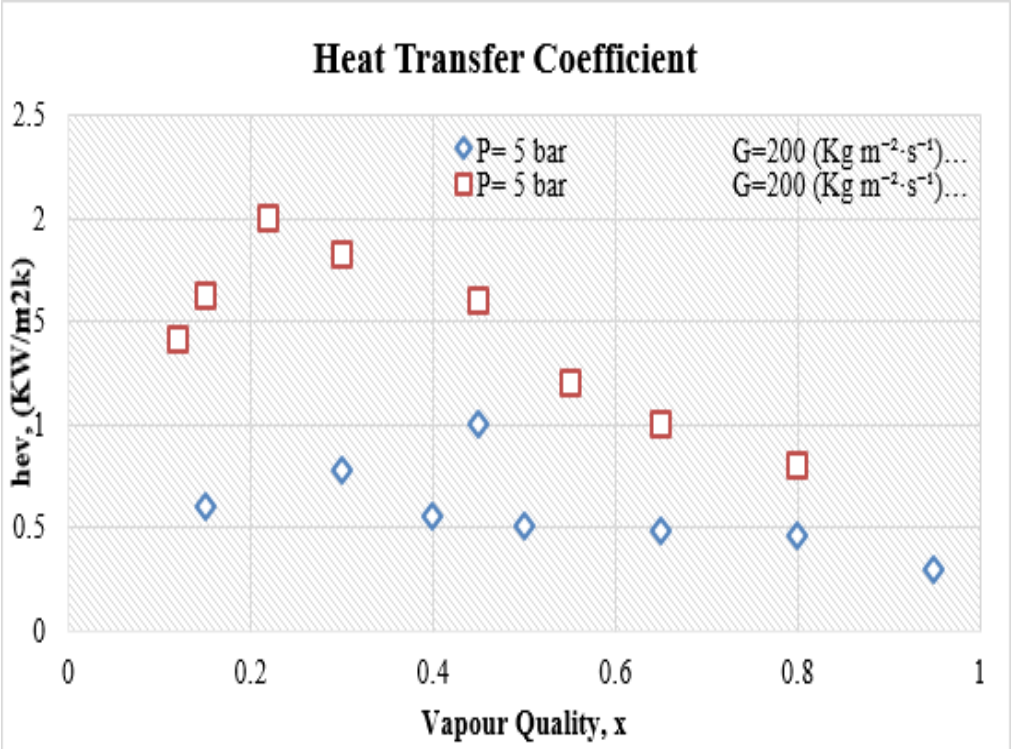

Figure 16: Heat Transfer Coefficient vs. Vapour Quality for HEV conditions.

The graph shows two loads. At a steady pressure of 5 bar and a mass flow of 200 kg m⁻2·s⁺2, heat flux ranges from 1.5 to 4.5 kW m⁻2. The graph shows how heat transfer coefficient (HEV) affects vapor quality (X). According to this image, vapor quality affects heat transfer. Because vapor quality varies between states, heat transfer efficiency changes. The heat transfer efficiency continues to rise and the vapor quality improves at q = 4.5 (kW m⁻2), particularly after the 0.3 mark. q=2 (kW m⁻2), in contrast, fluctuates more; certain values decrease as vapour quality increases.

International Journal of Environmental Sciences
ISSN: 2229-7359
Vol. 11 No. 23s, 2025
https://theaspd.com/index.php

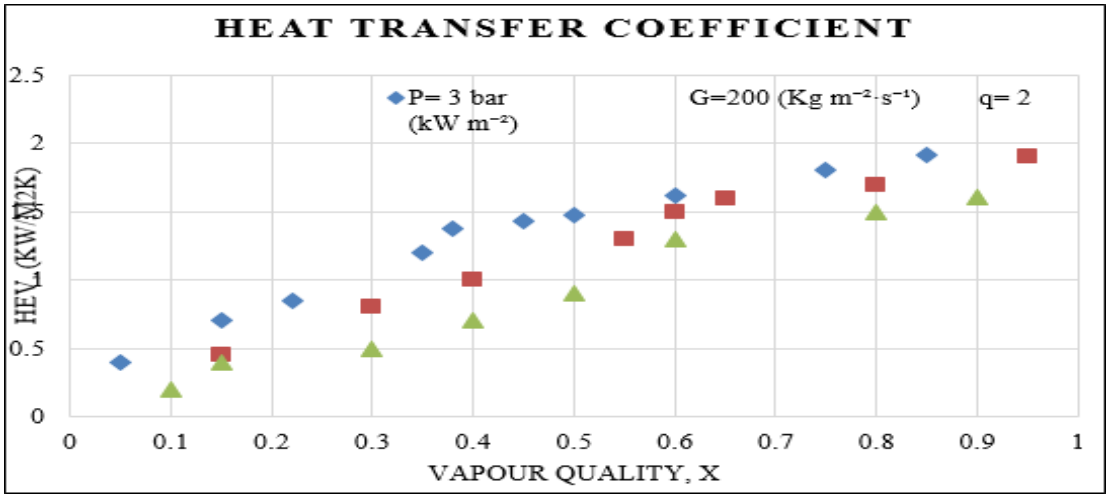

Figure 17: Heat Transfer Coefficient vs Vapour Quality

In three stages at 3, 5, and 7 bar pressure, the figure shows vapor quality (X) and heat transfer coefficient (HEV, kW/m2·K) fluctuations. The heat flux continues at 2 kW m⁻2, whereas the mass flow remains at 200 kg m⁻2·s⁻*. Air quality improves with heat transfer coefficient, the study found. Whenever the heat transfer coefficient is below 0.2, air quality stays poor at around 0.5 kW/m2·K. With air quality ranging from 0.2 to 0.5, heat transfer coefficients reach 1.5 kW/m2·K. The heat transfer coefficient changes at 0.5. The green and orange phases peak at 0.9 and 0.75, respectively, while the blue phase continues to rise. Air quality rating is near 1, about 2.0 kW/m2·K, with greatest heat transfer coefficient at 3 bar pressure. Gas quality affects the heat transfer coefficient, and different phases behave differently even under the same circumstances.

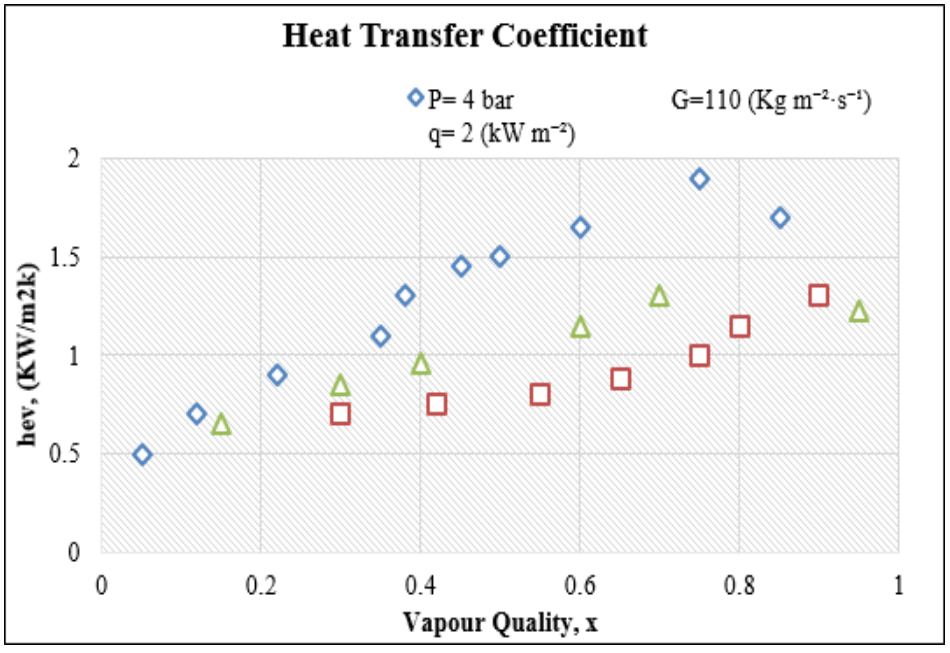

Figure 18: Heat Transfer Coefficient vs Vapour Quality

The air quality (X) and heat transfer rate (HEV, kW/m2·K) are shown in this picture. The pressure is 4 bar, and the mass flow is 110, 155, or 200 kg m⁻2·s⁻*. The heat flow stays the same at 2 kW m⁻2. Here are the numbers for the different heat transfer factors (G): The G numbers are 110, 155, and 200. This number is low when the gas quality is bad (0.05 to 0.2), and it's between 0.5 and 0.9. The heat transfer coefficient starts to rise more noticeably when the air quality goes above 0.3. The optimal values are between the range of 0.7 and 0.9. In one scenario, a gas quality of 0.75 results in the maximum heat transfer efficiency. Following this, the coefficient either remains constant or gradually decreases until it reaches a value of around 1.23 at a vapor quality of 0.95.

International Journal of Environmental Sciences
ISSN: 2229-7359
Vol. 11 No. 23s, 2025
https://theaspd.com/index.php

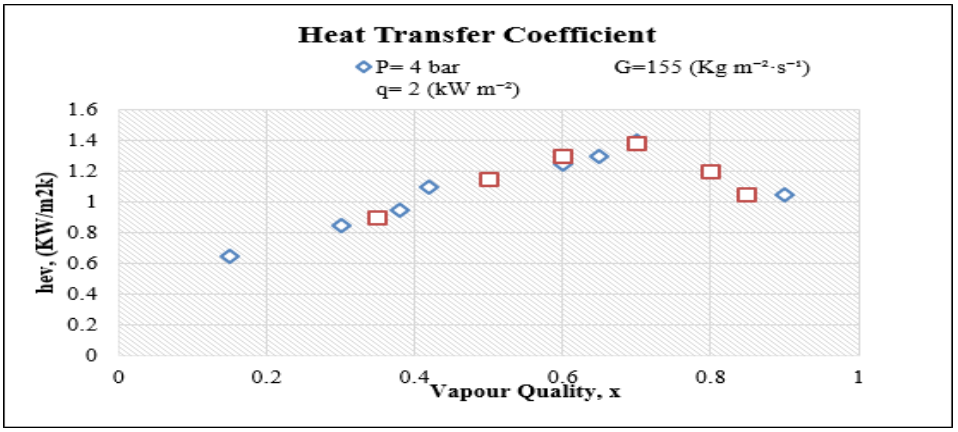

Figure 19: Heat Transfer Coefficient vs Vapour Quality

The heat transfer coefficient (HEV) and vapor quality (X) both evolve over time. Both q = 2 (kW m⁻2) and q = 4 (kW m⁻) at 4 bar pressure are shown in the photo. Improvements in gas quality lead to an improvement in HEVs. Given q = 2 (kW m⁻2), the HEV value may be anywhere between 0.65 kW/m2·K and 1.4 kW/m2·K. When the air quality improves, the values of HEVs increase from 1.2 kW/m2·K to 1.38 kW/m2·K for q = 4. More heat is being conveyed when the gas quality is greater, as the HEV values are somewhat higher for q = 4 (kW m⁺2) compared to q = 2 (kW m⁺2).

Part B: Investigation of Heat Transfer Enhancement in R-407C Evaporation using Twisted Tape Turbulent Promoters

Comparative study of twisted tape

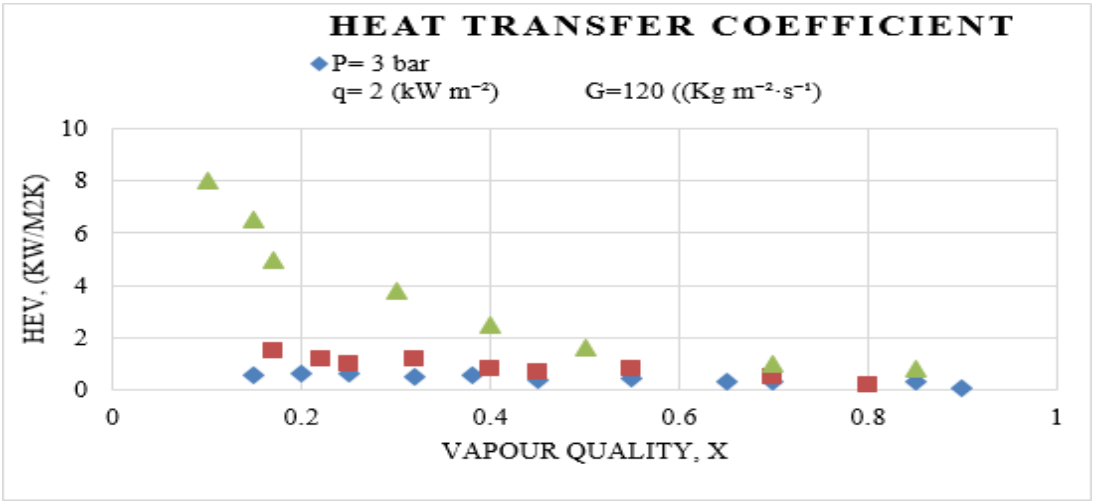

Figure 20: Heat Transfer Coefficients of Twisted Tape Inserts at Different Operating Conditions (Twist Ratio 7)

This study tests how well R-407C moves heat in a straight tube with tape pieces that are bent out of shape. They change when there are three different working conditions: (i) pressures of 3, 5, and 7 bar; (ii) heat fluxes of 2, 4.5, and 7kW/m2; and (iii) mass fluxes of 120, 210, and 280 kg/m2.s; and a rotation ratio of 7. The data shows that the heat transfer coefficient isn't very high when the quality of the gas is low (X < 0.4), and it changed a lot between three and five bar lower pressures. As the quality of the gas gets better (X < 0.8), the heat transfer coefficient always goes up. At 7 bar of pressure, however, there is an interesting change: the heat transfer coefficient almost doubles between X = 0.0 and 0.5. From these results, it seems likely that as pressure and mass flow rise, heat transfer will become more efficient.

International Journal of Environmental Sciences
ISSN: 2229-7359
Vol. 11 No. 23s, 2025
https://theaspd.com/index.php

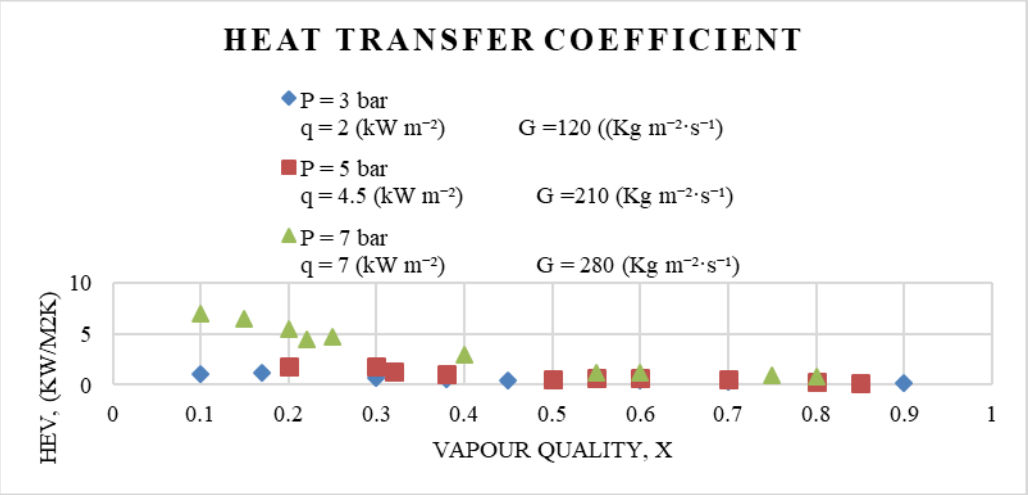

Figure 21: Comparative Study of Heat Transfer Performance for R-407C in a Horizontal Tube with Twisted Tape Inserts at Different Operating Conditions (Twist Ratio S)

When comparing the heat transfer performance of R-407C in a horizontal tube with twisted tape inserts, the results demonstrated that experimental heat transfer coefficients changed for pressures of 3, 5, and 7 bar, heat fluxes of 2, 4.5, and 7 kW/m^2, & mass fluxes of 120, 210, and 280 kg/m^2·s. The twisting ratio for the combinations was eight to one. If the air quality is bad (X < 0.4), the heat transfer coefficient will be lower and both pressures might fluctuate. But these patterns seem different at 3 bar. When the pressure was 5 bars, the results were similar. Larger pressure and better air quality were found to make the heat transfer rate much higher. The most productive workers were those who manipulated factors related to the strength and clarity of the gas. Generally, using curled tape pieces made it easier for heat to pass through.

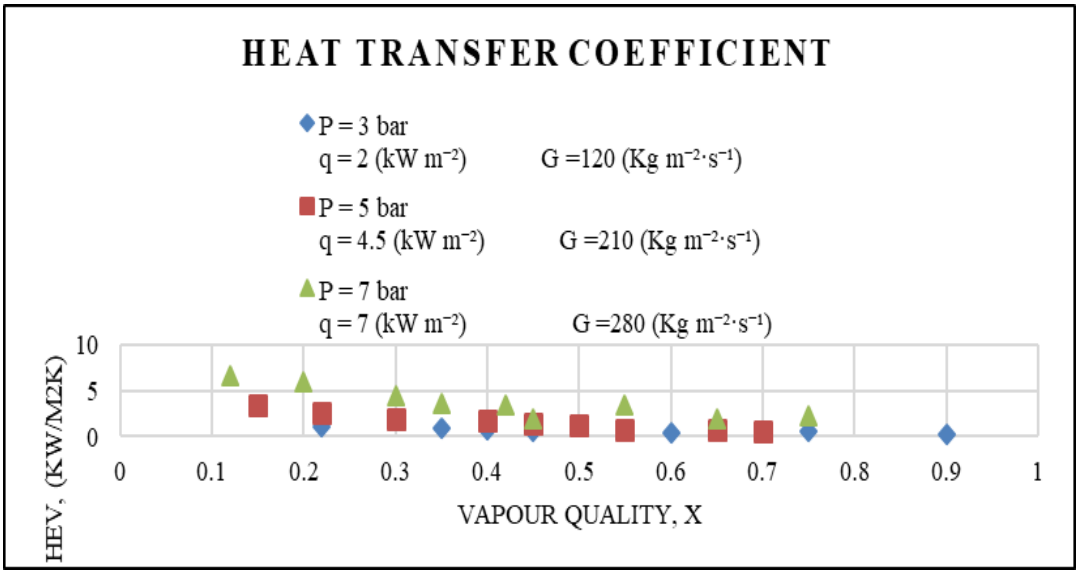

Figure 22: Comparative Study of Heat Transfer Performance for R-407C in a Horizontal Tube with Twisted Tape Inserts at Different Operating Conditions (Twist Ratio 9)

HEV graph for R-407C in flat tube with twisting tape inserts: 3, 5, and 7 bar pressures, 2, 4.5, and 7 kW/m2 heat flows, 120, 210, and 280 kg/m2·s mass flows. The graph demonstrates how gas quality affects HEV at various pressures and mass flow rates.

International Journal of Environmental Sciences
ISSN: 2229-7359
Vol. 11 No. 23s, 2025
https://theaspd.com/index.php

Comparative Performance

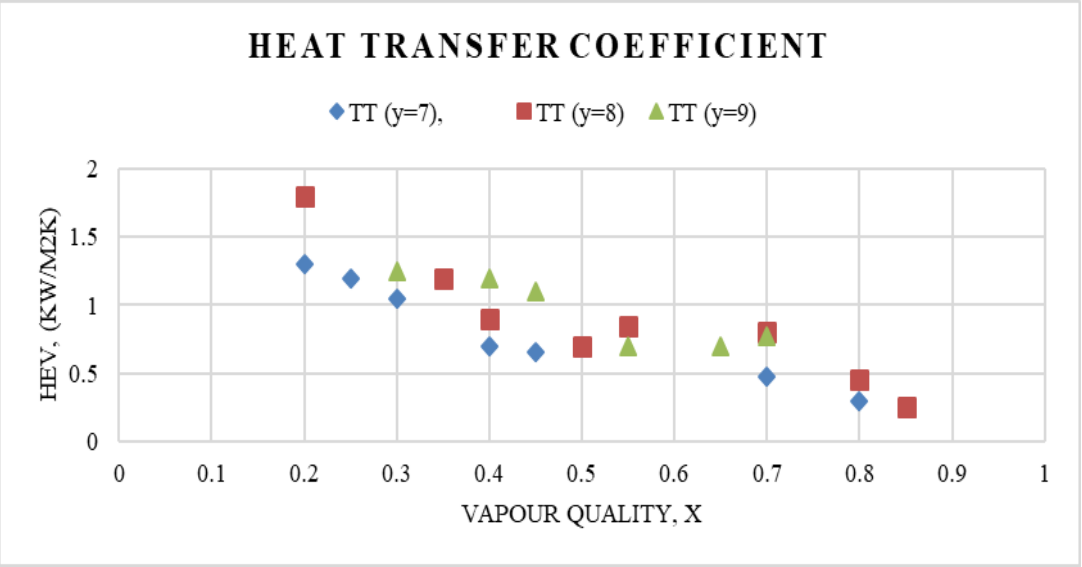

Figure 23: Comparative Performance of Heat Transfer Coefficients for Different Vapour Qualities

A horizontal tube with twisted tape inserts was used to test R-407C's efficacy. There was a pressure of 3 bar, a mass flow of 120 kg/m2·s, and a heat flow of 2 kW/m2. As a result, the connection between X, the air quality index, and HEV was shown. When X fell below 0.4, the heat transfer coefficient fluctuated between 0.25 and 1.25 kW/m2·K. At a vapor quality of 0.2, the coefficient reached 1.8 kW/m2·K, but it dropped to 0.4 as the vapor quality increased. The results showed that better gas properties led to better heat transfer efficiency. This was especially true between 0.4 and 0.7, which is when the HEV and heat efficiency were at their highest.

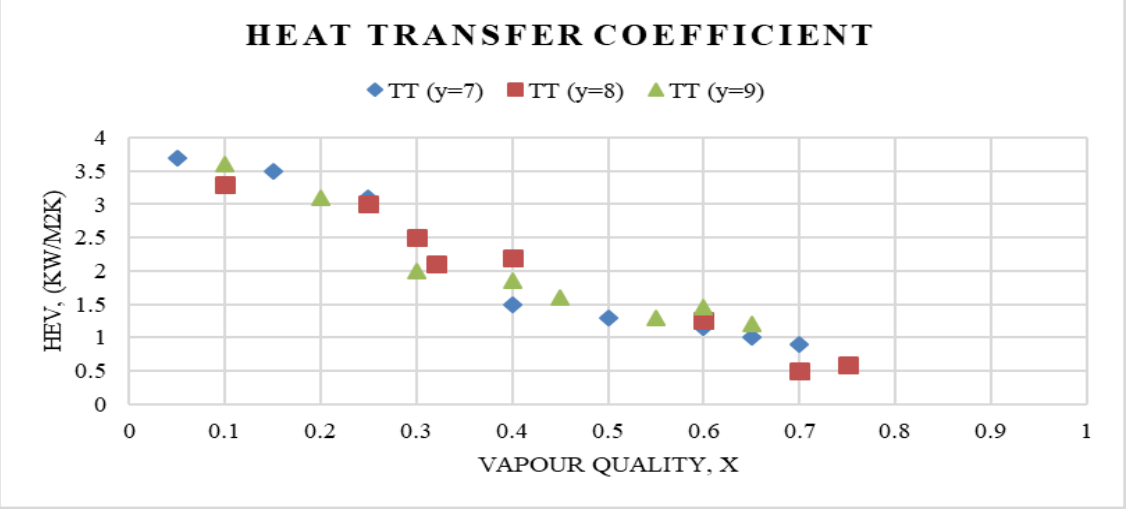

Figure 24: Heat Transfer Performance of R-407C with Twisted Tape Inserts

The link between vapor quality (X) and heat transfer coefficient (HEV) in twisted tape-inserted horizontal tubes was explored. The mass flow was 210 kg/m2·s, heat flux was 4.5 kW/m2, and pressure was 5 bar. leads indicate that poor air quality (X < 0.4) leads in low heat transfer coefficients (1.0 to 3.7 kW/m2·K). Increasing vapor quality raises the number continually. This is especially true when vapor quality rises to X=0.4. The highest value achieved was 3.6 kW/m2·K at X=0.1. Heat transfer coefficients plateau and decline until reaching 1.45 kW/m2·K at X = 0.6. For medium-quality and pressure vapors, heat efficiency improves.

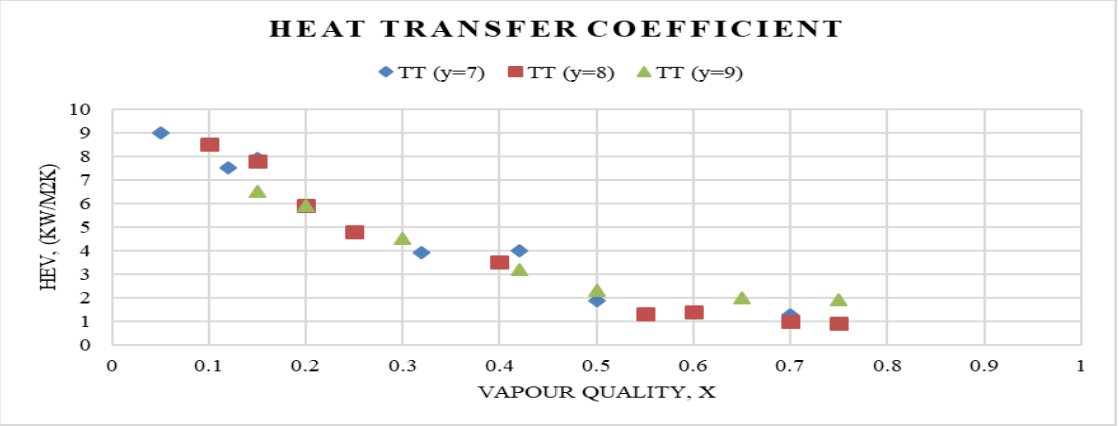

Figure 25: Heat Transfer Performance of R-407C with Twisted Tape Inserts at 7 Bar Pressure

This graph displays the R-407C's performance in a horizontal tube with twisted tape inserts. Under the following conditions: 7 bar pressure, 7 kW/m2 heat flux, and 280 kg/m2·s, the relationship between vapor quality (X) and heat transfer coefficient (HEV) is shown in the chart. A high heat transfer coefficient (3.9-9 kW/m2·K) was linked to poor vapor quality (X < 0.4), as per the investigation. After falling at X = 0.4, the heat transfer coefficient reaches a plateau at 1.87 kW/m2.K as soon as the air quality surpasses 0.4. As the vapor quality increases, this pattern indicates that heat transmission is decreased.

Comparative study of Perforated twisted tape

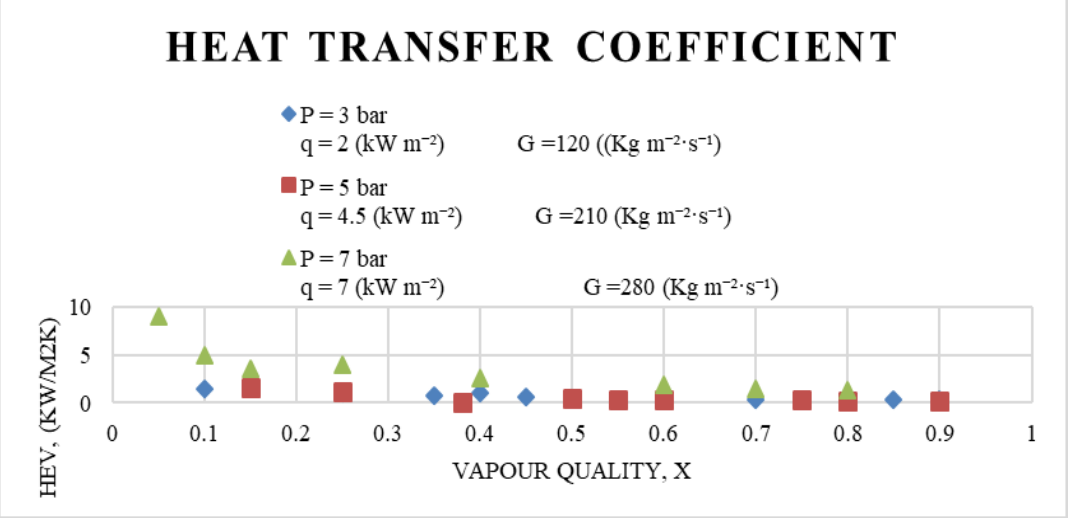

Figure 26: Heat Transfer Performance of R-407C with Twisted Tape Inserts at Various Pressures and Heat Fluxes (Twist Ratio 7)

Using twisted tape inserts, the R-407C runs in a horizontal tube as seen in the figure. At3,5, and 7 bar, the heat transfer coefficient (HEV) and vapor quality (X) are shown to be related at 2,4.5, and 7 kW/m2 and 120,210, and 280 kg/m2·s, respectively, for mass fluxes. When X is less than 0.4, the heat transfer coefficient is low in the range of 0.25 to 1.65 kW/m2·K. The heat transfer coefficient grows exponentially with gas quality at pressures of 5 and 7 bars in particular. In air with a quality of0.6, the heat transfer coefficient was greatest, indicating that R-407C was a good heat conductor.

International Journal of Environmental Sciences
ISSN: 2229-7359
Vol. 11 No. 23s, 2025
https://theaspd.com/index.php

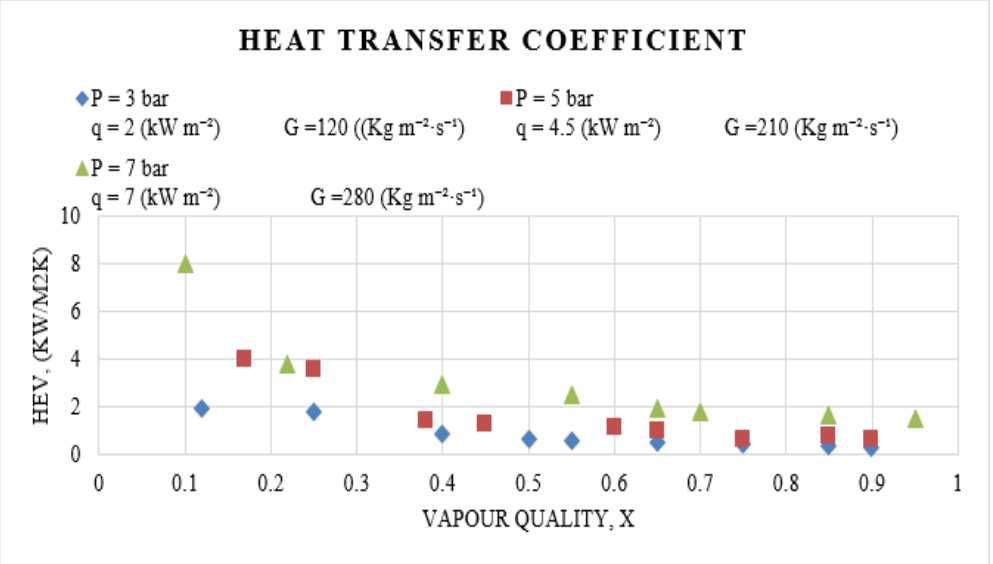

Figure 27: Heat Transfer Performance of R-407C with Twisted Tape Inserts at Various Pressures and Heat Fluxes (Twist Ratio 8)

R-407C is seen in the image operating inside a horizontal tube that has twisted tape inserts. The relationship between vapor quality (X) and heat transfer coefficient (HEV) at3,5, and 7 bar (in bars). The data for mass flow (120, 210, as 280 kg/m2·s) & heat flux (2, 4.5, and 7 kW/m2) are also made available. Data shows low heat transfer coefficient in poor air quality (X < 0.4). It varied from 0.3 to 1.95 kW/m2·K. Gas quality improved heat transfer coefficient primarily at 5 and 7 bar pressures. The heat transfer coefficient rose fast to X = 0.9. Greater vapor quality tends to boost heat transfer efficiency. Seven bar was the only pressure with high medium vapor quality HEV values.

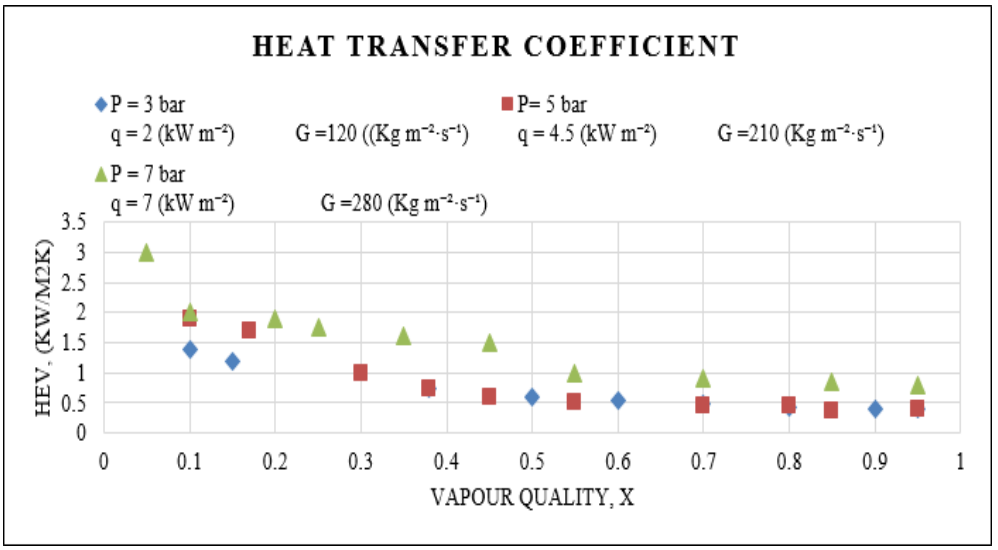

Figure 28: Heat Transfer Performance of R-407C with Twisted Tape Inserts at Various Pressures and Heat Fluxes (Twist Ratio 9)

R-407C uses twisted tape inserts to operate in a horizontal tube. Heat transfer coefficient (HEV) and vapor quality (X) at 3, 5, and 7 bar are shown on a graph. While the mass flows are 120, 210, and 280 kg/m2·s, the heat fluxes are 2, 4.5, and 7 kW/m2. When the air quality is poor (X < 0.4), the heat transfer coefficient is low (0.38-3 kW/m2·K). Gas quality has a significant impact on HEV, particularly at 5 and 7 bar. The heat transfer coefficient increases when X = 0.9, enhancing air quality and thermal performance.

Comparative Performance

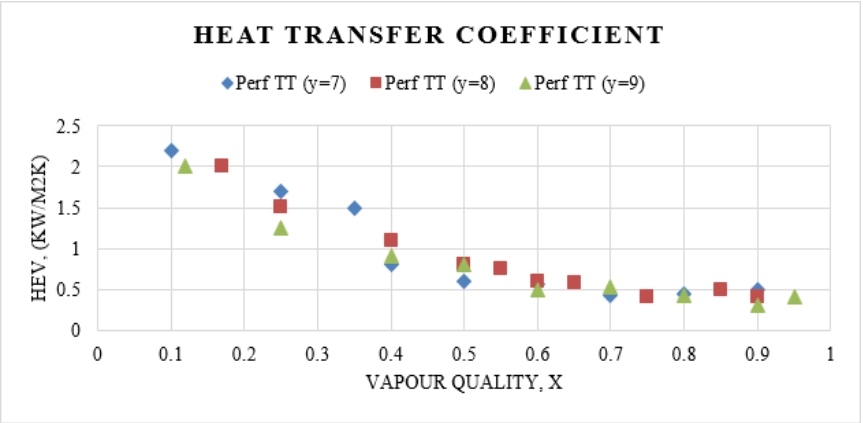

Figure 29: Comparative Performance of R-407C with Twisted Tape Inserts at 3 Bar Pressure and Varying Heat Flux and Mass Flux

This figure shows the performance of R-407C in a horizontal tube with twisted tape inserts at 3 bar of pressure, 2 kW/m2 of heat flow, and 120 kg/m2·s of mass flow. Low air quality (X < 0.4) results in a lower heat transfer coefficient (HEV). It falls between 0.3 and 2.2 kW/m2·K. Improved gas quality, especially when X = 0.4, results in a drop in HEV. The value drops to at least 0.3 kW/m2·K when X equals 0.9. While effectiveness declines with increasing vapor quality, the heat transfer coefficient rises. In these circumstances, better air quality may have prevented heat transfer.

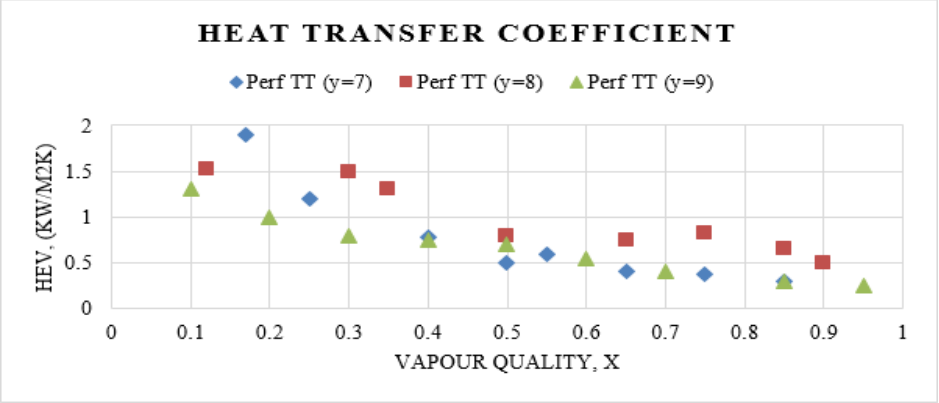

Figure 30: Comparative Performance of R-407C with Twisted Tape Inserts at 5 Bar Pressure and Varying Heat Flux and Mass Flux

At a pressure of 5 bar, a heat flow of 4.5 kW/m2, and a mass flow of 210 kg/m2·s, the image illustrates the efficacy of R-407C in a straight conduit using twisted tape inserts. The heat transfer index (HEV) ranges from 0.25 to 1.9 kW/m2·K when X is less than 0.4. The HEV appeared to be the most detrimental at X = 0.95. It experienced a gradual decline as the purity of the gas improved, particularly between X = 0.5 and 0.75. This demonstrates that the design effectively disseminated heat through the air. The efficiency of heat transfer was reduced as a result of the improvement in air quality. Heat is more effectively conserved, and the quality of the gas is consistent.

VI. DISCUSSION

Various conditions are tested in each round of the study to determine the heat transfer efficiency of R-407C in a horizontal tube with and without twisted tape inserts. The evaporation heat transfer rate, pressure drop, and temperature glide were recorded in Part A of the experiment. poor gas quality resulted in poor heat transfer coefficient (X < 0.4) in flow bubbling results. Heat transfer coefficient rose with gas purity, especially at 6 and 8 bar pressure. This pattern suggests that pressure improves heat transmission, particularly with higher-quality gas. This must be considered while developing heat transfer usage. The findings from part B's turbulence booster work with twisted tape inserts showed significant heat transfer improvements. Between 0.25 and 1.65 kW/m2·K, heat transfer efficiency was poor (X < 0.4). Similar to

these findings, values improved and even sextupled at 5 bar and 7 bar pressures. The peak was obtained at 7 bar pressure, with a gain of around 9 kW/m2·K and X = 0.05. These findings offer us hope that the twisted tapes insert would affect heat transport, particularly under pressure, but we need additional investigation. The heat transfer coefficient decreases as gas quality increases (X > 0.75). This may be because the vapor quality region switches from nucleate boiling to other boiling, making heat transport less effective at higher vapor qualities. Even though these statistics are lower, twisted tape inserts' research shows that they increase heat transmission by 35 to 45%. They also improved evaporative heat transfer greatest.

Table 7: Percentage Increase in Local Heat Transfer Coefficient with Perforated Twisted Tape Inserts at Different Operating Conditions

Operating Set	Operating Condition	Vapor Quality (X)	% Increase in Local Heat Transfer Coefficient	Plain Tube	Twisted Tape	Perforated Twisted Tape
1	P = 3 bar, q = 2 kW/m2, G = 120 kg/m2·s	Around 0.25	25.45	40.5	30.5	56.8
		Around 0.4	42.35	56.8	48.2	75.2
		Around 0.5	58.9	75.2	60.3	60.8
		Around 0.7	41.67	60.8	51.2	55.3
2	P = 5 bar, q = 4.5 kW/m2, G = 210 kg/m2·s	Around 0.2	35.6	55.3	44.1	69
		Around 0.4	49.7	69	55.4	52.4
		Around 0.6	30.55	52.4	43.3	45
		Around 0.8	26.8	45	38	90
3	P = 7 bar, q = 7 kW/m2, G = 280 kg/m2·s	Around 0.05	63	90	75.5	92.5
		Around 0.25	85.8	92.5	87.1	63.9
		Around 0.45	41.2	63.9	55.7	68.8
		Around 0.6	50.6	68.8	62.8	56.8

VII CONCLUSION

From the experimental results, the following inferences can be derived:

- Higher operating pressure promotes heat transfer. As pressure increases, the heat transfer coefficient rises in the area with poorer vapor quality (X = 0.1 to 0.4) then declines until 0.6 or 0.7. Mass transfer resistance increases with vapor quality, slowing heat transmission. This indicates nucleate boiling ceases at 0.4 vapor quality.
- Mass flow increases with heat transfer coefficient. Particularly for low-quality clouds between 0.05 and 0.3. There are few nucleation sites, therefore boiling ceases rapidly. This improves heat transmission in low-air-quality areas.
- Heat transmission efficiency increases with a mist grade of 0.4 or above. When air quality diminishes, nucleate boiling prevents wall temperature rise. This reduces wall superheating and increases heat flow.
- Gas quality often leads to an increase in temperature. Temperature drops somewhat when air quality is between 0.3 and 0.65. R-407C flows and boils without R32, the less volatile portion. As the stable mixture grows, the temperature increases quicker.

- The data demonstrates the complex link between working circumstances and heat transfer efficiency. They demonstrate how pressure, mass flow, and vapor quality must be optimized in R-407C systems for optimal heat transfer.

VIII. REFERENCES

[1] L. Cremaschi and S. Moghaddam, 'Recent advances on heat and mass transfer in refrigeration and air-conditioning systems', Sci. Technol. Built Environ., vol. 23, no. 6, pp. 871–874, Aug. 2017, doi: 10.1080/23744731.2017.1334502.

[2] G. Geum et al., 'Thermal performance analysis of heat pipe heat exchanger for effective waste heat recovery', Int. Commun. Heat Mass Transf., vol. 151, p. 107223, Feb. 2024, doi: 10.1016/j.icheatmasstransfer.2023.107223.

[3] S. Hasan Ibrahim and H. A. Abdul Wahhab, 'Influence of Twisted Tape Inserts with Perforation on Heat Transfer and Pressure Drop Inside Circular Tube: Numerical and Experimental Investigation', in ICPER 2020, F. Ahmad, H. H. Al-Kayiem, and W. P. King Soon, Eds., in Lecture Notes in Mechanical Engineering. , Singapore: Springer Nature Singapore, 2023, pp. 281–293. doi: 10.1007/978-981-19-1939-8_24.

[4] B. Kumar Ahirwar and A. Kumar, 'A comprehensive review on heat transfer enhancement in tubular heat exchangers using twisted tapes, wire coil inserts, and their combined effect with nanofluids', Renew. Sustain. Energy Rev., vol. 224, p. 116035, Dec. 2025, doi: 10.1016/j.rser.2025.116035.

[5] A. R. S. Suri, A. Kumar, and R. Maithani, 'Convective heat transfer enhancement techniques of heat exchanger tubes: a review', Int. J. Ambient Energy, vol. 39, no. 7, pp. 649–670, Oct. 2018, doi: 10.1080/01430750.2017.1324816.

[6] M. A. Rahman, S. M. M. Hasnain, and R. Zairov, 'Assessment of improving heat exchanger thermal performance through implementation of swirling flow technology', Int. J. Thermofluids, vol. 22, p. 100689, May 2024, doi: 10.1016/j.ijft.2024.100689.

[7] L. Yuan, S. Zou, Y. Yang, and S. Chen, 'Boundary-Layer Disruption and Heat-Transfer Enhancement in Convection Turbulence by Oscillating Deformations of Boundary', Phys. Rev. Lett., vol. 130, no. 20, p. 204001, May 2023, doi: 10.1103/PhysRevLett.130.204001.

[8] M. D. Hambarde, R. Shrivastava, S. R. Thorat, and O. P. Dale, 'Experimental investigation on evaporation of R407C in a single horizontal smooth tube', IRA-Int. J. Technol. Eng. ISSN 2455-4480, vol. 7, no. 2 (S), p. 266, Jul. 2017, doi: 10.21013/jte.ICSESD201726.

[9] M. D. Hambarde and R. Shrivastava, 'Heat transfer Enhancement against Void Fraction in Flow Boiling of R407C using Twisted Tapes', vol. 8, no. 1, 2019.

[10] Hambarde, 'Comparative study of heat transfer performance of twisted tape inserts in evaporation of r407c', 2018, [Online]. Available: https://scholar.google.com/citations?view_op=view_citation&hl=en&user=T5jgNMMAAAAJ&citation_for_view=T5jgNMMAAAAJ:Se3iqnhoufwC

[11] K. Bilen, K. Dağıdır, and E. Arcaklıoğlu, 'experimental investigation of effects of nanorefrigerants on vapor compression refrigeration system using R1234yf INSTEAD OF R134a', Isı Bilimi Ve Tek. Derg., vol. 44, no. 2, pp. 280–293, Nov. 2024, doi: 10.47480/isibted.1563896.

[12] S. Deb et al., 'Flow boiling heat transfer characteristics over horizontal smooth and microfin tubes: An empirical investigation utilizing R407c', Int. J. Therm. Sci., vol. 188, p. 108239, Jun. 2023, doi: 10.1016/j.ijthermalsci.2023.108239.

[13] A. Diani and L. Rossetto, 'R1234ze(E) Flow Boiling inside a 2.5 mm ID Smooth Tube and Comparison against an Equivalent Microfin Tube', Appl. Sci., vol. 11, no. 6, p. 2627, Mar. 2021, doi: 10.3390/app11062627.

[14] G. A. Mancin, Simone, G. Righetti, and C. Zilio, 'Comparative analysis of microfin vs smooth tubes in R32 and R410A boiling', Int. J. Refrig., vol. 131, pp. 515–525, Nov. 2021, doi: 10.1016/j.ijrefrig.2021.06.005.

[15] H. Nalbandian, C.-Y. Yang, and K.-T. Chen, 'Flow Boiling Heat Transfer of Refrigerants HFO-1234yf and HFC-134a in an Extruded Aluminum Tube with Multi-Port microchannels', Int. J. Refrig., vol. 142, pp. 37–47, Oct. 2022, doi: 10.1016/j.ijrefrig.2022.06.013.

[16] N. K. Vidhyarthi et al., 'Influence of Microfin Tube on Heat Transfer during Flow Boiling of R134a Refrigerant', J. Eng., vol. 2024, no. 1, p. 6824128, Jan. 2024, doi: 10.1155/2024/6824128.

[17] H. Nalbandian, C.-Y. Yang, and K.-T. Chen, 'Flow Boiling Heat Transfer of Refrigerants HFO-1234yf and HFC-134a in an Extruded Aluminum Tube with Multi-Port microchannels', Int. J. Refrig., vol. 142, pp. 37–47, Oct. 2022, doi: 10.1016/j.ijrefrig.2022.06.013.

[18] C. Dang and Y. Nakamura, 'Boiling heat transfer of HFO-1234yf flowing in a smooth small-diameter horizontal tube', Int. J. Refrig., vol. 34, no. 8, pp. 1846–1853, Dec. 2011, doi: 10.1016/j.ijrefrig.2011.05.018.

[19] T. Saito, 'experimental clarification of gas-liquid interaction in turbulence generated by using an oscillating-grid', 2011.

[20] G. A. Longo, S. Mancin, G. Righetti, and C. Zilio, 'R1234yf and R1234ze(E) as environmentally friendly replacements of R134a: Assessing flow boiling on an experimental basis', Int. J. Refrig., vol. 108, pp. 336–346, Dec. 2019, doi: 10.1016/j.ijrefrig.2019.09.008.

[21] D. F. Sempértegui-Tapia and G. Ribatski, 'Flow boiling heat transfer of R134a and low GWP refrigerants in a horizontal micro-scale channel', Int. J. Heat Mass Transf., vol. 108, pp. 2417–2432, May 2017, doi: 10.1016/j.ijheatmasstransfer.2017.01.036.

[22] Z. Yang, W. Chen, and M. K. Chyu, 'Numerical study on the heat transfer enhancement of supercritical CO2 in vertical ribbed tubes', Appl. Therm. Eng., vol. 145, pp. 705–715, Dec. 2018, doi: 10.1016/j.applthermaleng.2018.09.081.

[23] C.-H. Li, N.-W. Kim, J.-I. Yoon, S.-H. Seol, and Joon-Hyuk, 'Evaporation Heat Transfer and Pressure Drop of Low-Global Warming Potential Refrigerant HFO-1234yf in 6.95-mm Horizontal Smooth Tube', Energies, vol. 14, no. 19, p. 6325, Oct. 2021, doi: 10.3390/en14196325.

[24] J. Zhang et al., 'R410A flow boiling in horizontal annular channels of enhanced tubes, part I: Pressure drop', Int. J. Refrig., vol. 137, pp. 70–79, May 2022, doi: 10.1016/j.ijrefrig.2022.02.009.

[25] X. Zhang et al., 'Experimental study of the nonisothermal gas-liquid two-phase heat transfer characteristics in a rectangular helical channel', Exp. Therm. Fluid Sci., vol. 163, p. 111393, Apr. 2025, doi: 10.1016/j.expthermflusci.2024.111393.

[26] G. Li et al., 'Stratification and heat transfer characteristics for R32-partially miscible oil mixture flow boiling inside a micro-fin tube', Int. J. Refrig., vol. 168, pp. 109–121, Dec. 2024, doi: 10.1016/j.ijrefrig.2024.08.005.
[27] S. Jadhav, M. Hambarde, R. Shrivastava, and G. Nandan, 'Pressure drop prediction in flow boiling of R-407C in two phase flow using twisted tape insert in horizontal tube', presented at the MATERIALS, MECHANICS & MODELING (NCMMM-2020), Jamshedpur, India, 2021, p. 030033. doi: 10.1063/5.0050373.
[28] S. Tarabkhah, B. Sajadi, and M. A. A. Behabadi, 'Prediction of heat transfer coefficient and pressure drop of R1234yf and R134a flow condensation in horizontal and inclined tubes using machine learning techniques', Int. J. Refrig., vol. 152, pp. 256–268, Aug. 2023, doi: 10.1016/j.ijrefrig.2023.04.031.
[29] Z. Li, J. Zhang, and Y. He, 'Experimental study on R410A flow boiling heat transfer outside three enhanced tubes with different fin structures', AIP Adv., vol. 10, no. 11, p. 115105, Nov. 2020, doi: 10.1063/5.0024157.